A 20 million-year Great Ediacaran Glaciation witnessed the rise of the earliest animals

Ruimin Wang (2001110607@pku.edu.cn)
School of Earth and Space Sciences, Peking University
Bing Shen
Peking University
Xianguo Lang
Chengdu University of Technology https://orcid.org/0000-0001-7698-4139
Bin Wen
School of Earth Sciences, China University of Geosciences, Wuhan
Haoran Ma
Peking University https://orcid.org/0000-0002-2899-484X
Zongjun Yin
State Key Laboratory of Palaeobiology and Stratigraphy, Nanjing Institute of Geology and Palaeontology, Chinese Academy of Sciences https://orcid.org/0000-0002-9391-0446
Yongbo Peng
Nanjing University https://orcid.org/0000-0001-6458-5552
Yonggang LIU
Peking University https://orcid.org/0000-0001-8844-2185
Chuanming Zhou
Nanjing Institute of Geology and Palaeontology and Center for Excellence in Life and Palaeoenvironment, Chinese Academy of Sciences

Article

Keywords: Ediacara biota, Great Ediacaran Glaciation, evolution,

Posted Date: October 21st, 2021

DOI: https://doi.org/10.21203/rs.3.rs-793746/v1

Abstract

Occurrence of Ediacara biota soon after the Gaskiers glaciation at ~ 580 Ma (million years ago) implies a possible glacial fuse of animal evolution[1,2]. To test this hypothesis, it is essential to resolve the spatial-temporal distributions of these Ediacaran glacial deposits. Here, we report the presence of globally synchronous ~ 570 – 560 Ma Shuram excursion, the largest negative carbonate carbon isotope excursion in Earth history[3,4], stratigraphically below the Ediacaran Hankalchough glacial deposits in the Tarim Block, confirming a post-560 Ma glaciation. Considering the wholesale rotation of the solid Earth (crust and mantle) via an inertial interchange true polar wander process from ca. 590 – 580 to 560 Ma[5–8], we observe that mapped Ediacaran glacial deposits were distributed on nearly all continents but were restricted roughly to mid-to-high latitudes. Thus, we propose a unique mid-to-high-latitude-dominated 'Great Ediacaran Glaciation' (GEG), lasting for more than 20 million years. The GEG bracketed the evolutionary window of Ediacara biota, implying an icehouse background for the rise of animals.

Main Text

Climate models predict that low-latitude glaciations, i.e., ice sheets extending to the sea level in tropical regions, occurred under the 'Snowball Earth' climatic condition, during which the Earth's surface was completely or mostly frozen for tens of million years [9,10]. Geochronological and paleomagnetic data confirm two Snowball Earth glaciations: the Sturtian (717-660 Ma) and Marinoan (650-635 Ma), both during the Cryogenian Period [11,12]. In the mid- to late- Ediacaran, widespread glacial deposits have also been noted (Fig. 1a, Table S1) and even been mapped to the low latitudes [12]. However, the non-Snowball Earth Ediacaran glaciation is supported by the occurrence of Ediacara fossils shortly (within 5 million years) after the Ediacaran Gaskiers glaciation [13,14], which is followed by the flourish of macroscopic algae [15], acanthomorphic acritarchs [16], the White Sea Assemblage of Ediacara Biota [2], the earliest biomineralization (e.g., *Cloudina* and associated small shelly fossils) [17], and the earliest bilaterians [18,19] in the following 30 million years (Fig. 1b). On the other hand, high-precision radiometric ages from the Gaskiers glacial deposits in Newfoundland suggested a short-lived (~1 million years, 580.90-579.88 Ma) glaciation [1]. This timescale is inconsistent with a Snowball Earth condition, nor there is a typical cap carbonate atop the glacial deposit in most other localities. Therefore, the temporal-spatial distributions of Ediacaran glaciations have not yet been resolved in the context of a non-Snowball Earth climatic condition.

The debates of Ediacaran glaciations are largely attributed to the loose geochronological and biostratigraphic constraints on most Ediacaran glacial deposits (Fig. 1a). There is not enough evidence to determine the Ediacaran glaciations on other continents were synchronous with the Gaskiers glaciation (Table S1, Fig. 1a). Although unambiguous latest Ediacaran fossils (<550 Ma) have been discovered above the Zhengmuguan and Hongtiegou glacial deposits, these fossil records only place the minimum age constraints on the glaciations in North China and Chaidam Block [20,21] (Fig. 1a). As such, two pulse of Ediacaran glaciations at ~580 Ma and <560 Ma have been proposed [22]. Chemostratigraphic data from carbonate-dominated successions may provide additional age constraints on the Ediacaran glaciations [3]. The Ediacaran carbonate carbon isotope ($\delta^{13}C_{carb}$) chemostratigraphic framework is characterized by three negative excursions [4,23] (EN1-EN3, Fig. 1b). The third negative $\delta^{13}C_{carb}$ excursion (EN3) or the Shuram excursion (SE) represented the largest negative $\delta^{13}C_{carb}$ excursion in Earth's history and might have recorded a prominent oxidation of the Ediacaran ocean [3,24]. SE can be easily identified by its extremely low $\delta^{13}C_{carb}$ values (<-10‰), warranting its explicit chemostratigraphic correlation [24,25]. The SE in Oman and Canada was dated between 574.0 ± 4.7 Ma and 567.3 ± 3.0 Ma [26], and the astrochronological study further confined an identical duration of ~8 million years of the SE from four continents, confirming its global synchronicity between 570.2 ±1.1 Ma and 562.5 ±1.1 Ma [27].

In this study, we report the SE from the Shuiquan Formation that underlies the Hankalchough glacial deposits in the Tarim Block, northwestern China. The Neoproterozoic Quruqtagh Group of the Tarim Block contains three glacial deposits: the Beiyixi, Tereeken, and Hankalchough formations. The former two can be correlated with the Sturtian and Marinoan Snowball Earth glaciations, respectively [28,29]. The youngest Hankalchough glaciation was younger than 615 ± 6 Ma [30]. It conformably overlies the carbonate-dominated Shuiquan Formation and unconformably underlies the black shale of early Cambrian Xishanblac Formation [28], implying an Ediacaran-age of the Hankalchough glaciation (Figs. 2, S1, S2). We measured $\delta^{13}C_{carb}$ of the Shuiquan Formation from two sections. In the Mochia-Khutuk (MK) section, $\delta^{13}C_{carb}$ increases from -5‰ to ~0‰ in the basal 3 m, and sharply decreases to -10‰ within 1 m. Low $\delta^{13}C_{carb}$ values persist over the next 25 m. After a subsequent sharp increase, $\delta^{13}C_{carb}$ remains nearly invariant between -2‰ and 0‰ until the Hankalchough glacial deposits. In the Heishan-Zhaobishan (HZ) section, low $\delta^{13}C_{carb}$ of -10‰ begins at the base and continues for ~5 m, followed by a slow increase to ~0‰ in the rest of Shuiquan Formation (Fig. 2, see SI).

The persistently low $\delta^{13}C_{carb}$ values of ~-10‰ lasting for 25 m in MK and ~5 m in HZ (Fig. 2) resemble the SE (EN3) observed in other localities rather than the EN2 that might be correlated with the Gaskiers glaciation at ~580 Ma [25]. Compared with the idealized SE pattern that is characterized by a rapid $\delta^{13}C_{carb}$ decrease and a gradual recovery [24], $\delta^{13}C_{carb}$ profile dose not display the initial stage in HZ, while the recovery interval is not recorded in MK. The absence of SE recovery stage in MK might be attributed to the poor outcrop (thus unsampled) or the occurrence of a depositional hiatus. On the other hand, there are two possible reasons for the absence of the initial SE stage in HZ: (1) diachroneity of the base of Shuiquan Formation, i.e., carbonate deposition in the deeper HZ postdating that in MK, and (2) obscurity of the SE signal in deeper water sections, given the widespread $\delta^{13}C_{carb}$ depth gradient in the stratified Ediacaran ocean [31].

Correlation of the negative $\delta^{13}C_{carb}$ excursion in the Shuiquan Formation with the Shuram Excursion is also supported by three lines of other geological and geochemical evidence. (1) Similar to other SE sections, the Shuiquan Formation is dominated by limestone, representing the deposition in the shallow marine environment (See SI) [24]. (2) There is a positive correlation between $\delta^{13}C_{carb}$ and $\delta^{18}O$ (Figs. S5, S6) [24,25]. Notably, the negative $\delta^{13}C_{carb}$ excursion in both MK and HZ is associated with a concurrent decrease in $\delta^{18}O$ values (as low as -15‰), but $\delta^{18}O$ does not shift back during the SE recovery (Fig. 2). Such $\delta^{13}C_{carb}$ and $\delta^{18}O$ stratigraphic trends are similar to the SE in Siberia [32]. (3) Carbonate carbon and organic carbon isotopes ($\delta^{13}C_{org}$) are decoupled in the Shuiquan Formation with $\delta^{13}C_{org}$ irregularly varying between -25‰ and -30‰ during the SE [33] (Figs. 2, S6). Therefore, the presence of SE in the Shuiquan Formation implying the overlying Hankalchough glaciation younger than ca. 560 Ma.

The Hankalchough glaciation might be correlated with those in Saudi Arabia, Chaidam, North China, West Africa and Kalahari [22,34,35] (Fig. 1, Table S1), reflecting a >20 million years gap between the Gaskiers and those post-560 Ma glaciations (Fig. 1). However, the available geochronological data cannot resolve whether there were two episodes of glaciation at 580 Ma and <560 Ma, respectively, or was a continuous ice-age lasting for more than 20 million years (Fig. 1). Here, we propose that an inertial interchange true polar wander (IITPW) event (i.e., the entire crust and mantle rotated ~90° about the liquid outer core), from ca. 590-580 to 560 Ma [5-8,36], may be applied to constrain the nature of Ediacaran glaciation.

New paleogeographic maps were reconstructed in the context of late Ediacaran IITPW event (Fig. 3, See SI). Since the non-Snowball Earth condition precludes the low latitude Ediacaran glaciations [9,10], the two-glaciation scenario can be rejected by fail to place all glacial depositions in mid- to high- latitude regions in either 560 Ma or 580 Ma paleogeographic maps. The glacial deposits in South Australia (the Billy Springs and the Groles Hill formations) and Baltica (the Moelvand Mortensnes formations) are placed at tropics in both 580 Ma and 560 Ma maps (Fig. S8), arguing against the two-glaciation scenario. In contrast, these glacial deposits are located at mid-latitude in the 570 Ma map (Fig. 3b). In fact, glacial deposits from the Tanin to Starye Pechi formations in Siberia likely represent the 570 Ma glaciation [37]. Moreover, multiple episodes of short-lived glaciation separated by nonglacial intervals are not common in Earth's history, e.g., the Late Ordovician glaciation lasting for ~1 million years did not occur repeatedly [38].

Instead, a continuous Ediacaran glaciation is well consistent with the paleogeographic reconstructions during IITPW (Fig. 3). Together with the compiled ages of Ediacaran glacial deposits (Table S1), we propose that the spatial and temporal distributions of Ediacaran glaciations were mainly controlled by the rapid latitudinal change of continents during the IITPW event. The 590-580 Ma glaciations in Avalon, Laurentia and Amazonian occurred in mid-to-high latitudes (Fig. 3A). Absence of younger glacial deposits (i.e., post-580 Ma glaciations) in these continents was due to their rotating into tropics during IITPW (Figs. 3B, C). Both South Australia and Baltica first rotated away from and then moved back to tropics, leaving glacial deposits briefly around 570 Ma (Fig. 3B). The post-SE glaciations, including the Luoquan/Zhengmuguan in North China, Hongtiegou in Chaidam, Hankalchough in Tarim, Nudaus in Kalahari, Dhaiqa in Arabia and Aourz in west Africa (Table S1), were coincident with the rotation of these tropical continents to higher latitude at the end of IITPW event ~ 560 Ma (Fig. 3C), Our study indicates a continuous Ediacaran glaciation, collectively coiled the ‘Great Ediacaran Glaciation’ (GEG), with a minimum duration of 20 million years between 580 Ma and 560 Ma (Fig. 1), may resemble the Late Paleozoic and Cenozoic ice-ages [39,40]. In fact, the lower bound of GEG could significantly predate 580 Ma (Fig. 1), as indicated by pervasive glendonite deposition throughout the lower Doushantuo Formation below the 580 Ma EN2 in South China, indicating the persistent cold water condition before 580 Ma [41]. On the other hand, some Ediacaran glaciations might postdate 550 Ma or be of early Cambrian age, further extending the duration of GEG (Fig. 1). Similar to Phanerozoic high-latitude glaciations lasting 10s of millions years, ice-sheets in GEG might have extended to sub-tropics around 30°N/S (Fig. 3), suggesting a much stronger icehouse climate than Phanerozoic ice-ages.

GEG was temporally coincident with the evolutionary window of Ediacaran biota, which first evolved at ~575 Ma (the Avalon Assemblage) and diversified at ~560 Ma (the White Sea Assemblage), and also overlapped with the age of Weng’an biota (Fig. 1), suggesting a direct linkage between GEG and animal evolution. Indeed, GEG would have facilitated a long-term ocean oxygenation [42], as shown by SE that reflecting a massive oxidation of dissolved organic carbon (DOC) in the deep ocean [3,43]. How GEG triggered the ocean oxygenation remains unclear. It is plausible that GEG might have favored nutrients (e.g., phosphorus) recycling, allowing P accumulation in the surface ocean, and accordingly would persistently sustain high primary productivity and oxygenation in the atmosphere. High phosphorus supply during GEG is supported by the global phosphate deposition in late Ediacaran [44]. Therefore, an extended global cooling in late Ediacaran might have provided an evolutionary window of ≥ 20 million years for macroscopic organisms, leading to the eventual emergence of bilaterians and Cambrian explosion.

References

1 Pu, J. P., Bowring, S. A., Ramezani, J. & Myrow, P. Dodging snowballs: Geochronology of the Gaskiers glaciation and the first appearance of the Ediacaran biota. *Geology (Boulder)* **44**, 955-958, doi:10.1130/G38284.1 (2016).

2 Shen, B., Dong, L., Xiao, S. & Kowalewski, M. The Avalon explosion: Expansion and saturation of Ediacara morphospace. *Science* **319**, 81-84 (2008).

3 Fike, D. A., Grotzinger, J. P., Pratt, L. M. & Summons, R. E. Oxidation of the Ediacaran ocean. *Nature* **444**, 744-747, doi:10.1038/nature05345 (2006).

4 Zhu, M., Zhang, J. & Yang, A. Integrated Ediacaran (Sinian) chronostratigraphy of South China. *Palaeogeography, Palaeoclimatology, Palaeoecology* **254**, 7-61, doi:10.1016/j.palaeo.2007.03.025 (2007).

5 Mitchell, R. N. *et al.* Sutton hotspot: Resolving Ediacaran-Cambrian Tectonics and true polar wander for Laurentia. *American Journal of Science* **311**, 651-663, doi:10.2475/08.2011.01 (2011).

6 Robert, B. *et al.* Constraints on the Ediacaran inertial interchange true polar wander hypothesis: A new paleomagnetic study in Morocco (West African Craton). *Precambrian Research* **295**, 90-116, doi:https://doi.org/10.1016/j.precamres.2017.04.010 (2017).

7 Robert, B., Greff-Lefftz, M. & Besse, J. True Polar Wander: A Key Indicator for Plate Configuration and Mantle Convection During the Late Neoproterozoic. *Geochemistry, Geophysics, Geosystems* **19**, 3478-3495, doi:10.1029/2018gc007490 (2018).

8 Wen, B., Evans, D. A. D., Anderson, R. P. & McCausland, P. J. A. Late Ediacaran paleogeography of Avalonia and the Cambrian assembly of West Gondwana. *Earth and Planetary Science Letters* **552**, 116591, doi:https://doi.org/10.1016/j.epsl.2020.116591 (2020).

9 Hoffman, P. F., Kaufman, A. J., Halverson, G. P. & Schrag, D. P. A Neoproterozoic snowball Earth. *Science* **281**, 1342-1346 (1998).

10 Hoffman, P. F. *et al.* Snowball Earth climate dynamics and Cryogenian geology-geobiology. *Science Advances* **3** (2017).

11 Hoffman, P. F. & Li, Z.-X. A palaeogeographic context for Neoproterozoic glaciation. *Palaeogeography, Palaeoclimatology, Palaeoecology* **277**, 158-172, doi:10.1016/j.palaeo.2009.03.013 (2009).

12 Li, Z.-X., Evans, D. A. D. & Halverson, G. P. Neoproterozoic glaciations in a revised global palaeogeography from the breakup of Rodinia to the assembly of Gondwanaland. *Sedimentary Geology* **294**, 219-232, doi:http://dx.doi.org/10.1016/j.sedgeo.2013.05.016 (2013).

13 Hebert, C. L., Kaufman, A. J., Penniston-Dorland, S. C. & Martin, A. J. Radiometric and stratigraphic constraints on terminal Ediacaran (post-Gaskiers) glaciation and metazoan evolution. *Precambrian Research* **182**, 402-412, doi:10.1016/j.precamres.2010.07.008 (2010).

14 Bowring, S., Myrow, P., Landing, E., Ramezani, J. & Grotzinger, J. Geochronological constraints on terminal Neoproterozoic events and the rise of metazoans. *Geophysical Research Abstracts* **5**, 13219 (2003).

15 Xiao, S., Yuan, X., Steiner, M. & Knoll, A. H. Macroscopic carbonaceous compressions in a terminal Proterozoic shale: A systematic reassessment of the Miaohe biota, South China. *Journal of Paleontology* **76**, 347-376 (2002).

16 Liu, P. *et al.* High-resolution biostratigraphic and chemostratigraphic data from the Chenjiayuanzi section of the Doushantuo Formation in the Yangtze Gorges area, South China: Implication for subdivision and global correlation of the Ediacaran System. *Precambrian Research* **249**, 199-214, doi:http://dx.doi.org/10.1016/j.precamres.2014.05.014 (2014).

17 Hua, H., Chen, Z., Yuan, X., Zhang, L. & Xiao, S. Skeletogenesis and asexual reproduction in the earliest biomineralizing animal *Cloudina*. *Geology* **33**, 277-280 (2005).

18 Chen, Z., Zhou, C., Yuan, X. & Xiao, S. Death march of a segmented and trilobate bilaterian elucidates early animal evolution. *Nature* **573**, 412-415, doi:10.1038/s41586-019-1522-7 (2019).

19 Zhu, M., Zhuravlev, A. Y., Wood, R. A., Zhao, F. & Sukhov, S. S. A deep root for the Cambrian explosion: Implications of new bio- and chemostratigraphy from the Siberian Platform. *Geology* **45**, 459-462, doi:10.1130/g38865.1 (2017).

20 Shen, B., Xiao, S., Dong, L., Zhou, C. & Liu, J. Problematic macrofossils from Ediacaran successions in the North China and Chaidam blocks: implications for there evolutionary root and biostratigraphic significance. *Journal of Paleontology* **81**, 1396-1411 (2007).

21 Pang, K. *et al.* New Ediacara-type fossils and late Ediacaran stratigraphy from the northern Qaidam Basin (China): Paleogeographic implications. *Geology*, doi:10.1130/g48842.1 (2021).

22 Zhou, C., Yuan, X., Xiao, S., Chen, Z. & Hua, H. Ediacaran integrative stratigraphy and timescale of China. *Sci. China Earth Sci.* **62**, 7-24, doi:10.1007/s11430-017-9216-2 (2019).

23 Halverson, G. P., Hoffman, P. F., Schrag, D. P., Maloof, A. C. & Rice, A. H. N. Toward a Neoproterozoic composite carbon-isotope record. *Geological Society of America Bulletin* **117**, 1181-1207 (2005).

24 Grotzinger, J. P., Fike, D. A. & Fischer, W. W. Enigmatic origin of the largest-known carbon isotope excursion in Earth's history. *Nature Geosci* **4**, 285-292 (2011).

25 Tahata, M. *et al.* Carbon and oxygen isotope chemostratigraphies of the Yangtze platform, South China: Decoding temperature and environmental changes through the Ediacaran. *Gondwana Research* **23**, 333-353, doi:10.1016/j.gr.2012.04.005 (2013).

26 Rooney, A. D. *et al.* Calibrating the coevolution of Ediacaran life and environment. *Proc Natl Acad Sci U S A* **117**, 16824-16830, doi:10.1073/pnas.2002918117 (2020).

27 Gong, Z. & Li, M. Astrochronology of the Ediacaran Shuram carbon isotope excursion, Oman. *Earth and Planetary Science Letters* **547**, 116462, doi:https://doi.org/10.1016/j.epsl.2020.116462 (2020).

28 Xiao, S. *et al.* The Neoproterozoic Quruqtagh Group in eastern Chinese Tianshan: Evidence for a post-Marinoan glaciation. *Precambrian Research* **130**, 1-26 (2004).

29 Shen, B. *et al.* Carbon, sulfur, and oxygen isotope evidence for a strong depth gradient and oceanic oxidation after the Ediacaran Hankalchough glaciation. *Geochimica et Cosmochimica Acta* **75**, 1357-1373, doi:http://dx.doi.org/10.1016/j.gca.2010.12.015 (2011).

30 Xu, B. *et al.* SHRIMP zircon U–Pb age constraints on Neoproterozoic Quruqtagh diamictites in NW China. *Precambrian Research* **168**, 247-258, doi:https://doi.org/10.1016/j.precamres.2008.10.008 (2009).

31 Jiang, G., Kaufman, A. J., Christie-Blick, N., Zhang, S. & Wu, H. Carbon isotope variability across the Ediacaran Yangtze platform in South China: Implications for a large surface-to-deep ocean δ13C gradient. *Earth and Planetary Science Letters* **261**, 303-320, doi:10.1016/j.epsl.2007.07.009 (2007).

32 Pokrovskii, B. G., Melezhik, V. A. & Bujakaite, M. I. Carbon, oxygen, strontium, and sulfur isotopic compositions in late Precambrian rocks of the Patom Complex, central Siberia: Communication 1. results, isotope stratigraphy, and dating problems. *Lithol Miner Resour* **41**, 450-474, doi:10.1134/s0024490206050063 (2006).

33 Swanson-Hysell, N. L. *et al.* Cryogenian Glaciation and the Onset of Carbon-Isotope Decoupling. *Science* **328**, 608-611, doi:10.1126/science.1184508 (2010).

34 Linnemann, U. *et al.* A ~565 Ma old glaciation in the Ediacaran of peri-Gondwanan West Africa. *International Journal of Earth Sciences* **107**, 885-911, doi:10.1007/s00531-017-1520-7 (2018).

35 Chumakov, N. M. The Baykonurian glaciohorizon of the Late Vendian. *Stratigraphy and Geological Correlation* **17**, 373-381, doi:10.1134/S0869593809040029 (2009).

36 McCausland, P. J. A., Hankard, F., Van der Voo, R. & Hall, C. M. Ediacaran paleogeography of Laurentia: Paleomagnetism and 40Ar–39Ar geochronology of the 583Ma Baie des Moutons syenite, Quebec. *Precambrian Research* **187**, 58-78, doi:https://doi.org/10.1016/j.precamres.2011.02.004 (2011).

37 Maslov, A. V. *et al.* New constraints for the age of Vendian glacial deposits (Central Urals). *Doklady Earth Sciences* **449**, 303-308, doi:10.1134/S1028334X13030203 (2013).

38 Finnegan, S. *et al.* The Magnitude and Duration of Late Ordovician–Early Silurian Glaciation. *Science* **331**, 903-906, doi:10.1126/science.1200803 (2011).

39 Fielding, C. R. *et al.* Stratigraphic imprint of the Late Palaeozoic Ice Age in eastern Australia: a record of alternating glacial and nonglacial climate regime. *Journal of the Geological Society* **165**, 129-140, doi:10.1144/0016-76492007-036 (2008).

40 Ehlers, J. & Gibbard, P. L. The extent and chronology of Cenozoic Global Glaciation. *Quaternary International* **164-165**, 6-20, doi:https://doi.org/10.1016/j.quaint.2006.10.008 (2007).

41 Wang, Z. *et al.* Wide but not ubiquitous distribution of glendonite in the Doushantuo Formation, South China: Implications for Ediacaran climate. *Precambrian Research* **338**, 105586, doi:https://doi.org/10.1016/j.precamres.2019.105586 (2020).

42 Evans, S., Diamond, C., Droser, M. & Lyons, T. Dynamic oxygen and coupled biological and ecological innovation during the second wave of the Ediacara Biota. *Emerging Topics in Life Sciences* **2**,

ETLS20170148, doi:10.1042/ETLS20170148 (2018).

43 Rothman, D. H., Hayes, J. M. & Summons, R. E. Dynamics of the Neoproterozoic carbon cycle. *Proceedings of the National Academy of Sciences of the United States of America* **100**, 8124-8129 (2003).

44 Cook, P. J. & Shergold, J. H. *Phosphate deposits of the world, Volume 1, Proterozoic and Cambrian Phosphorites*. (Cambridge University Press, 1986).

45 Xiao, S. H. *et al.* Towards an Ediacaran Time Scale: Problems, Protocols, and Prospects. *International Union of Geological Sciences* **39**, 540-555, doi:10.18814/epiiugs/2016/v39i4/103886 (2016).

46 Xiao, S. H. & Narbonne, G. M. in *Geologic Time Scale 2020* (eds Felix M. Gradstein, James G. Ogg, Mark D. Schmitz, & Gabi M. Ogg) 521-561 (Elsevier, 2020).

Declarations

Acknowledgments:

We thank Chengqing Li, Ran He, and Tianzheng Huang for field assistant.

Funding:

This study was supported by the National Natural Science Foundation of China [grant numbers 41772359].

Author contributions

Conceptualization: BS

Methodology: RW, BW, HM and YP,

Investigation: RW and BW

Visualization: RW and BW

Funding acquisition: BS

Writing – original draft: RW, BS

Writing – review & editing: BS, BW, RW, ZY, YL, CZ and XL

Competing interests:

Authors declare that they have no competing interests.

Data and materials availability:

All data are available in the main text or the supplementary materials.

Supplementary Materials

Supplementary Text

Figs. S1 to S9

Tables S1 to S5

Figures

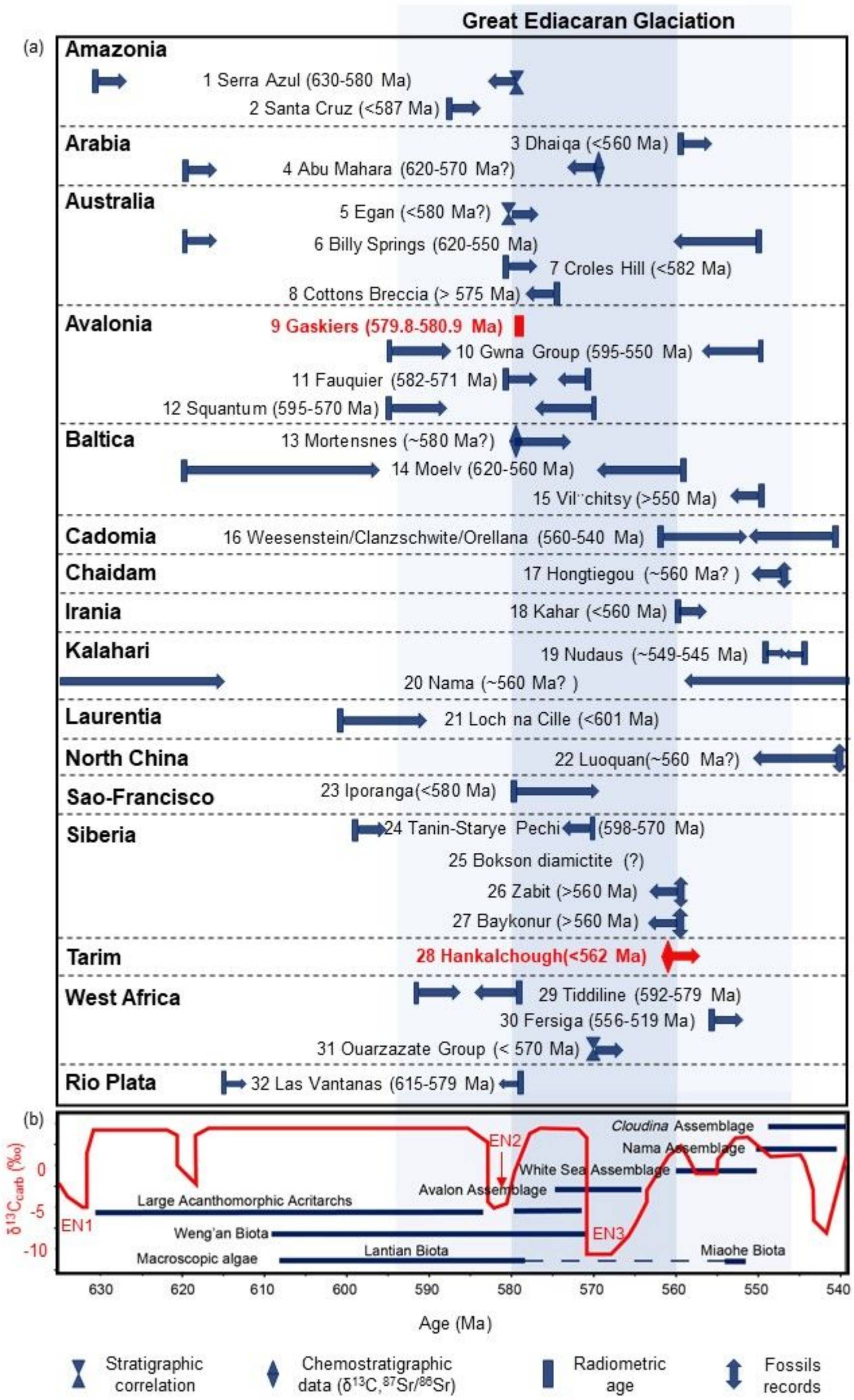

Figure 1

Temporal distributions of Ediacaran glacial deposits, biological evolution, and carbonate carbon isotope chemostratigraphy of Ediacaran Period. (a) The age constraints of Ediacaran glacial deposits in different continents. The age constraints are derived from radiometric dating, chemostratigraphy, biostratigraphy and regional stratigraphic correlation, and are listed in Table S1 (see the evaluations and references herein). Precise age constraints in Gaskiers Formation of Avalonia and in Hankalchough Formation of

Tarim (this study) are marked in bold red. The dark shadow indicates the confirmed range, while the light shadow marks the possible extended range of the Great Ediacaran Glaciation. (b) The Ediacaran carbonate carbon isotope chemostratigraphy (red line) and typical Ediacaran fossil records 2,4,16,19,45,46.

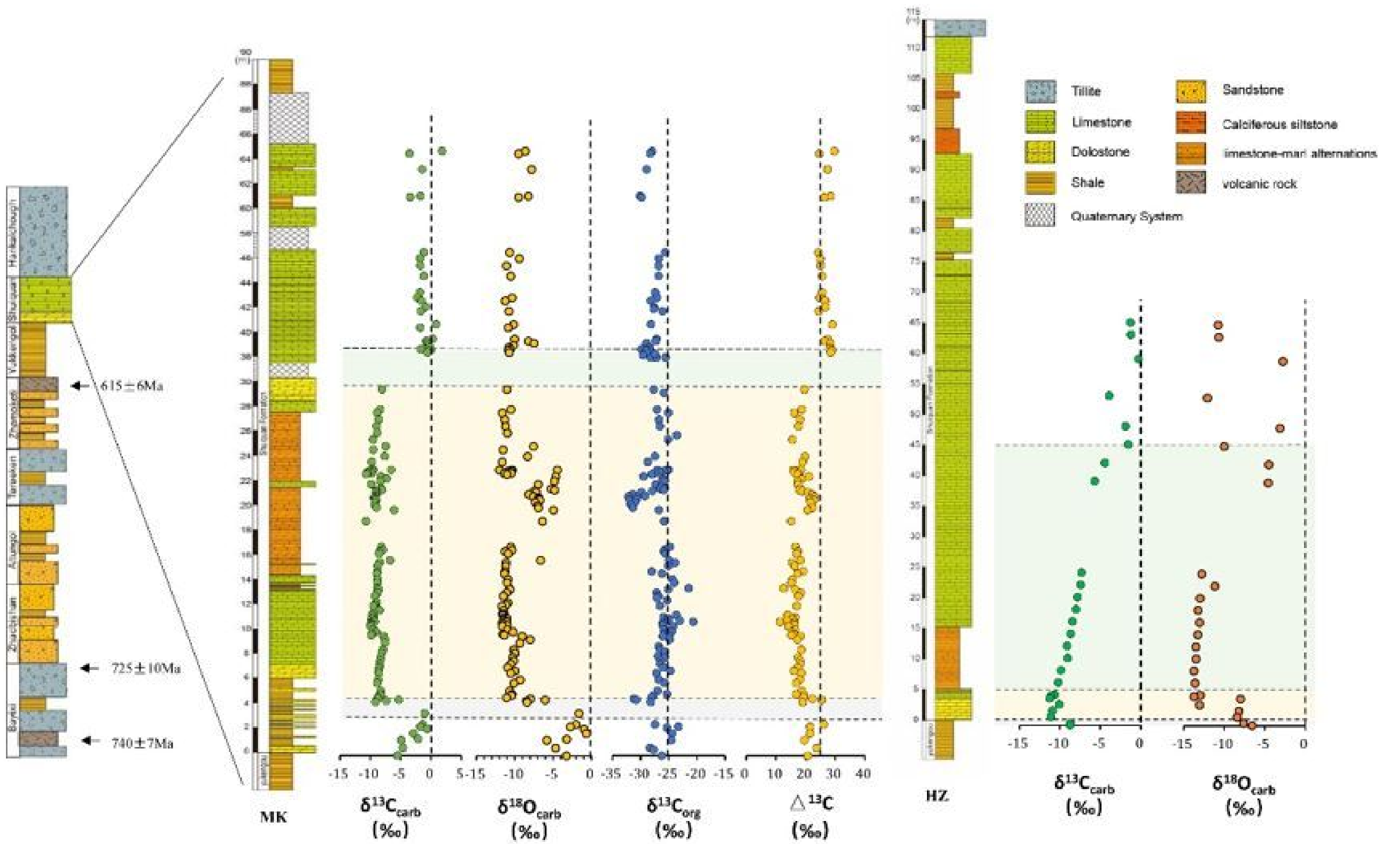

Figure 2

Chemostratigraphic profiles of the Shuiquan Formation at the Mochia-Khutuk (MK) and Heishan-Zhaobishan (HZ) sections. A prominent δ13Ccarb negative excursion to -10‰, the decoupling of δ13Ccarb and δ13Corg, and the concurrent negative excursion in δ18O indicate the Shuram excursion below the Hankalchough glacial deposits.

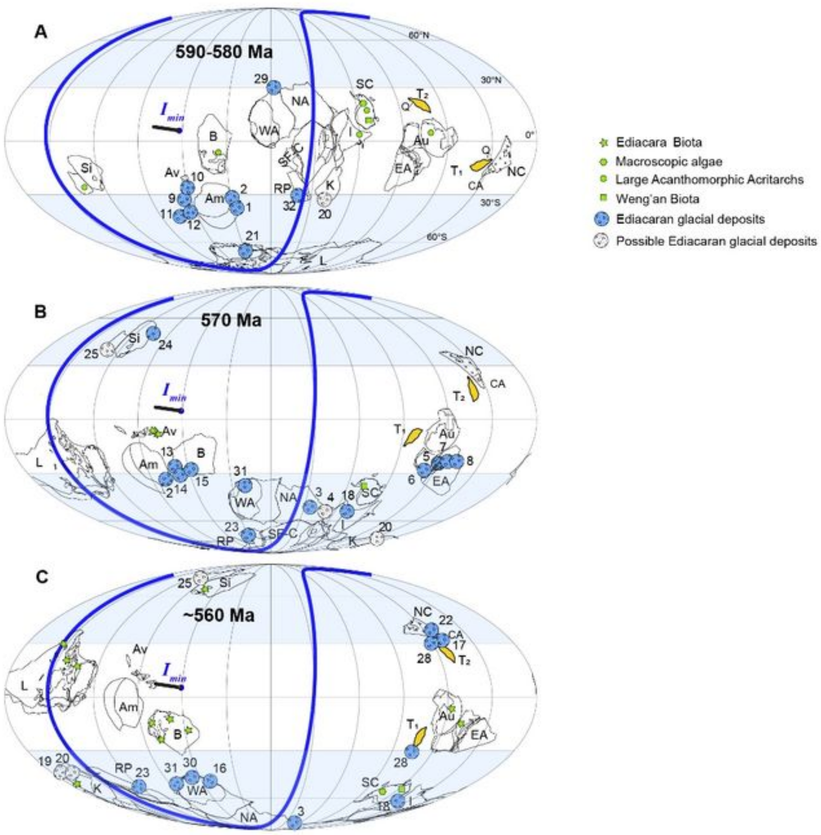

Figure 3

Different segments of spatial-temporal distributions for the prolonged (≥20 Ma) Ediacaran glaciation in an absolute framework from ca. 590-580 to 560 Ma. Imin, the minimum-inertial moment axis, about which the entire solid Earth rotated during the inertial interchange true polar wander (IITPW) event. It is calculated as the pole to the great circle (blue) by fitting the 590-560 Ma paleopoles (See SI, Fig. S7). Two (T1, T2) positions for the Tarim Block are consider (See more details for the reconstruction in

Supplementary files). Glacial deposits are numbered, and are listed in Fig 1 and Table S1. The Ediacaran fossil records are marked by different green symbols 2,19,45,46. NC-North China, T-Tarim, CA-Chaidam, Au-Australia, EA- East Antarctica, WA-West Africa, NA-Northeast Africa (Ab-NA), I-India, SC-South China, SFC-Sao Francisco-Congo, RP-Rio Plata, K-Kalahari, B-Baltica, Am-Amazonia, Av-Avalonia, Si- Siberia, L-Laurentia.

Supplementary Files

This is a list of supplementary files associated with this preprint. Click to download.

- WangEGNatureSI.pdf